Published as: *J Pathol*. 2013 September ; 231(1): .

Mutations in Hedgehog pathway genes in fetal rhabdomyomas

Simone Hettmer[1,2,3,*], **Lisa A Teot**[4], **Paul van Hummelen**[5], **Laura MacConaill**[5], **Roderick T Bronson**[6], **Claudia Dall'Osso**[1], **Junhao Mao**[7], **Andrew P McMahon**[8], **Peter J Gruber**[9], **Holcombe E Grier**[3], **Carlos Rodriguez-Galindo**[3], **Christopher D Fletcher**[10], and **Amy J Wagers**[1,2]

[1]Howard Hughes Medical Institute, Department of Stem Cell and Regenerative Biology, Harvard University, Harvard Stem Cell Institute, Cambridge, MA, USA

[2]Joslin Diabetes Center, Cambridge, MA, USA

[3]Department of Pediatric Oncology, Dana–Farber Cancer Institute and Division of Pediatric Hematology/Oncology, Boston Children's Hospital, MA, USA

[4]Department of Pathology, Boston Children's Hospital, MA, USA

[5]Center for Cancer Genome Discovery, Dana–Farber Cancer Institute, Boston, MA, USA

[6]Department of Biomedical Sciences, Tufts University Veterinary School, North Grafton, MA, USA

[7]University of Massachusetts Medical School, Worcester, MA, USA

[8]Department of Stem Cell Biology and Regenerative Medicine, Keck School of Medicine of the University of Southern California, Los Angeles, CA, USA

[9]Division of Cardiothoracic Surgery, University of Utah School of Medicine, Salt Lake City, UT, USA

[10]Department of Pathology, Brigham and Women's Hospital, Boston, MA, USA

Abstract

Ligand-independent, constitutive activation of Hedgehog signalling in mice expressing a mutant, activated *SmoM2* allele results in the development of multifocal, highly differentiated tumours that express myogenic markers (including desmin, actin, MyoD and myogenin). The histopathology of these tumours, commonly classified as rhabdomyosarcomas, more closely resembles human fetal rhabdomyoma (FRM), a benign tumour that can be difficult to distinguish from highly differentiated rhabdomyosarcomas. We evaluated the spectrum of Hedgehog (HH) pathway gene mutations in a cohort of human FRM tumours by targeted Illumina sequencing and fluorescence *in*

*Correspondence to: S Hettmer, Department of Pediatric Oncology, Dana–Farber Cancer Institute and Division of Pediatric Hematology/Oncology, Boston Children's Hospital, Boston, MA 02115, USA. simone.hettmer@childrens.harvard.edu.

No conflicts of interest were declared.

Author contributions

SH, CDF and AJW conceived experiments; SH and PVH carried out experiments; SH, LAT, PVH, RTB and CDF analysed data; and SH, LAT, PVH, LM, RTB, CD, JM, AM, PJG, HEG, CRG, CDF and AJW interpreted data. All authors were involved in the writing of the manuscript and had final approval of the submitted manuscript.

SUPPORTING INFORMATION ON THE INTERNET

The following supplementary material may be found in the online version of this article:

Table S1. Age of human tissue specimens surveyed, quality control measures and sequencing metrics

Table S2. List of non-synonymous SNVs in human FRMs

Table S3. List of indels observed in human FRMs

Table S4. OncoPanel coverage of Hedgehog pathway genes *PTCH1*, *SMO*, *SUFU* and *HIP1*

situ hybridization testing for *PTCH1*. Our studies identified functionally relevant aberrations at the *PTCH1* locus in three of five FRM tumours surveyed, including a *PTCH1* frameshift mutation in one tumour and homozygous deletions of *PTCH1* in two tumours. These data suggest that activated Hedgehog signalling contributes to the biology of human FRM.

Keywords

fetal rhabdomyoma; hedgehog signalling; *PTCH1*

Introduction

Hedgehog (HH) signalling is essential in many developmental processes [1] and has been linked to the development of a variety of malignant neoplasms, including rhabdomyosarcoma [2,3]. HH binds to the transmembrane receptor Patched 1 (Ptch1) to relieve inhibition of the transmembrane signal transducer Smoothened (Smo). Activated Smo then mediates proteolytic processing of the Gli family of zinc finger transcription factors to drive transcription of downstream target genes, including *Ptch1* and *Gli1* (negative and positive components of the HH feedback system) [1,4] (Figure 1B). Mice that are haploinsufficient for the HH receptor *Ptch1* [5] or for the HH binding protein *Hip1* [6], both negative regulators of HH signalling, and mice that express an activated *Smo* allele (*SmoM2*; Figure 1A) [4] are prone to develop tumours with myogenic differentiation, commonly classified as embryonal rhabdomyosarcomas [4–6]. Our review of the histopathology of *SmoM2* rhabdomyosarcomas revealed that these tumours show prominent cytodifferentiation, lack nuclear atypia and closer resemble human fetal rhabdomyomas (FRM). Human FRMs are rare benign tumours that typically arise in children and younger adults, have a predilection to occur at head/neck sites, occasionally infiltrate into adjacent normal skeletal muscle and can be complicated by local recurrence [7–9]. They do not cause regional or systemic metastases, and their ultimate outcome is benign [7]. Multifocal FRMs have been described in the context of nevoid basal cell carcinoma syndrome (NBCCS; a genetic disorder linked to *PTCH1* mutations) [8,10].

FRMs typically consist of bland spindle cells and elongated muscle cells reminiscent of fetal myotubules in a fibromyxoid stroma (Figure 3A) [7], and their lack of nuclear atypia and low mitotic rate serves as a distinguishing feature between FRM and rhab-domyosarcoma. However, overlap in the histological presentation of human FRM and highly differentiated human rhabdomyosarcoma has been well documented in the literature, and the distinction of human FRM from highly differentiated RMS can sometimes be problematic [7,9,11]. As HH-driven tumours with myogenic differentiation in mice with hyperactive HH signalling resemble human FRMs, we sought to investigate the molecular underpinnings and, specifically, the frequency of HH pathway gene mutations in these rare tumours. Our studies identified functionally relevant aberrations at the *PTCH1* locus in three of five human FRMs surveyed, including a frameshift mutation (g.98,220,305GC > G) in one tumour and homozygous deletions of *PTCH1* in two tumours. The frequent detection of PTCH1 inactivating mutations in human FRMs suggests that hyperactive HH signalling contributes to the development or maintenance of human FRMs.

Materials and methods

Mice

R26-SmoM2 (mixed genetic background, including 129/Sv and Swiss Webster as main components) and *CAGGS-CreER* mice were purchased from the Jack-son Laboratory. The mice were bred and maintained at the Joslin Diabetes Center Animal Facility. Tamoxifen (1

mg/40 g body weight; Sigma, St. Louis, MO, USA) was injected intraperitoneally on postnatal day 10 (P10) to induce Cre expression. Animals were monitored once weekly for the onset of soft-tissue tumours or other health problems, and were sacrificed once they had palpable muscle tumours or were ill. All animal experiments were approved by the Joslin Diabetes Center Institutional Animal Care and Use Committee.

Human tissue specimens

Human FRM specimens (FRM1-6) and corresponding normal tissue were obtained from the pathology archives at Boston Children's Hospital (FRM4-6) and the Brigham and Women's Hospital, Boston, MA (FRM1-3). Accurate histopathological diagnosis was verified by LAT and CDF. Corresponding normal tissue was available for tumours FRM5-6 only (CONO5-6). Discarded normal human skeletal muscle obtained from donors without tumour history (NO1-3) was obtained from PJG (see supplementary material, Table S1). All studies involving human tissue samples were approved by the relevant institutional review boards (Boston Children's Hospital, IRB-P00003845; Joslin Diabetes Center, CHS#06-42).

Histopathological evaluation of mouse *SmoM2* tumours

Tumours harvested from mice were fixed in 4% v/v paraformaldehyde for 2 h, embedded in paraffin, sectioned and stained with haematoxylin and eosin (H&E). For immunohistochemistry, 4 μm sections of paraffin-embedded tissue were baked, deparaffinized and subjected to heat-induced antigen retrieval in target retrieval solution, pH 9 (Dako, Carpinteria, CA, USA). The sections were then treated with peroxidase and protein blockers (Dako) and incubated with antibodies against myogenin (1:100; M3559; Dako), MyoD1 (1:50; M3512; Dako), desmin (1:50; M0760; Dako), actin (1:200, Dako M0635) and Ki67 (1:250; VP-K451; Vector Laboratories). The detection system was mouse Envision (Dako) for 30 min, followed by development with a 3,3V-diaminobenzidine chromagen substrate for 5 min. The slides were lightly counter-stained with haematoxylin. Isotype-specific antibodies were used as negative controls.

RT–PCR

Total RNA was isolated by TRIzol extraction and reverse-transcribed using Superscript I First-Strand Synthesis System for RT–PCR (Invitrogen, Carlsbad, CA, USA). qRT–PCR was performed using an AV7900 PCR system (Invitrogen) with Taqman PCR reagents. The primers used were Taqman Gene Expression *Gli1* (Mm00494654_m1), *Ptch1* (Mm00436026_m1) and *18s* (Mm03928990_g1).

DNA isolation and sequencing analysis of human tissue specimen

Genomic DNA was isolated from 10–15 punches (diameter 0.6 mm) obtained from formalin-fixed paraffin-embedded (FFPE) tissue blocks or from five unstained sections/specimen, using the DNeasy Blood and Tissue kit (Qiagen, Hilden, Germany). DNA was analysed using PICOgreen fluorescence to quantify double-stranded DNA. Total DNA yield was 61–816 and 51–2327 ng for FRM and normal tissue specimens, respectively. Of note, all FRM tissue samples were older than 10 years. Sequencing was performed using OncoPanel v.1, a targeted Illumina sequencing strategy of the coding regions of 645 genes previously linked to human cancer, including HH pathway genes *PTCH1*, *SMO*, suppressor of fused homologue (*SUFU*; acts as a negative regulator of HH signalling by downregulating *GLI1* -mediated transactivation of target genes) and *HIP1* [1]. Prior to library preparation, 51–200 ng DNA was fragmented by Covaris sonication to 150 bp and further purified using Agentcourt AMPure XP beads. 50 ng size-selected DNA was then ligated to sequencing adaptors with sample-specific barcodes during library preparation (Illumina TruSeq) and quantified by qPCR. The yields of the libraries were in the range 83–

2308 ng. The yield of the library obtained from sample FRM1 was only 3 ng, and this sample was discarded from further analysis. The remaining samples were pooled in equimolar concentrations to a total of 500 ng for targeted exon enrichment, using the OncoPanel v.1 gene set with the Agilent SureSelect hybrid capture kit, and sequenced in one lane for 100 bp paired-end reads/fragment on an Illumina Hiseq 2000. Pooled sample reads were deconvoluted (demultiplexed) and sorted using the Picard tools (for details, see: http://picard.sourceforge.net/command-line-overview.shtml). Reads were aligned to the reference sequence b37 edition from the Human Genome Reference Consortium, using bwa (http://bio-bwa.sourceforge.net/bwa.shtml) and the parameters '-q 5 -l 32 -k 2 -o 1'. Duplicate reads were identified and removed using the Picard tools. The alignments were further refined using the GATK tool for localized realignment around indel sites (http://www.broadinstitute.org/gsa/wiki/index.php/Local_realignment_around_indels). Recalibration of the quality scores was performed using GATK tools (http://www.broadinstitute.org/gsa/wiki/index.php/Base_quality_score_recalibration). The sequence generated a total of 482 330 586 reads and $43 \pm 5 \times 10^6$ reads/sample. Samples NO1-3 had high mean target coverages of ×232–284, while the tumour and matched normal samples only reached a mean target coverage of ×44–66. However, in all cases taken together, 63.4–90.2% of target bases were covered at least ×30, including 79% of Hedgehog (HH) gene-coding regions (see supplementary material, Table S4). Mutation analysis for single nucleotide variants (SNVs) was performed using MuTect v. 1 0.27200 (https://confluence.broadinstitute.org/display/CGATools/MuTect) and annotated by Oncotator (http://www.broadinstitute.org/oncotator), developed by the Cancer Biology Group at the Broad Institute. MuTect was made available through the generosity of Kristian Cibulskis and the Cancer Genome Analysis Program at the Broad Institute, Inc. Insertions and deletions (indels) were called using Indel Locator (https://confluence.broadinstitute.org/display/CGATools/Indelocator). We considered only those SNVs that were non-synonymous, detected in a tumour fraction > 30% (total pairs > 30, MQ0 < 10), corresponding to a 60% tumour purity, absent in normal muscle specimens NO1-3 and listed in the Exome Variant Server, NHLBI Exome Sequencing Project (ESP; Seattle, WA, USA) with a population frequency < 1%. We considered those indels found in an allele fraction > 25%.

Fluorescence *in situ* hybridization (FISH)

A two-colour FISH probe set was hybridized to 5 μm sections of seven paraffin-embedded tissue samples (FRM4-6, NO1-3, CONO5), including a custom-made probe for *PTCH1* (RP11-435O5, labelled with spectrum orange) and a commercial probe for *CEP9* (labelled with spectrum green). For tumours FRM2-3 and corresponding normal tissue CONO6, no remaining paraffin-embedded tissue was available for FISH testing.

Results

HH-driven myogenic tumours in *SmoM2* mice resemble human FRM

In *R26-SmoM2;CAGGS-CreER* mice, expression of a mutant, activated *Smo* allele (*SmoM2*) via an ubiquitously expressed transgene encoding a tamoxifen-inducible *Cre* recombinase (Figure 1A; *CAGGS-CreER*) resulted in hyperactivity of HH pathway signalling (Figure 1B) [4]. Tamoxifen-induced mice developed a spectrum of neoplasms, including tumours with myogenic differentiation previously classified as rhabdomyosarcomas (Figure 2) [4]. These tumours developed with high penetrance within the first 3 months of life (Figure 1C; 32 mice evaluated). The majority of tumours arose in the rear thigh, hindlimb and chest wall muscles, as previously described [4]. They were typically multifocal (average 4 ± 1 tumours/mouse detected; Figure 1D), and random skeletal muscle sections revealed numerous microscopic tumour foci (Figure 1F). Tumours reached considerable size (average 358 ± 67

mg total tumour mass/mouse; Figure 1D), but did not metastasize to the lungs of tumour-bearing animals. No metastatic foci were detected in random lung sections of 10 tumour-bearing mice. Expression of HH target genes *Ptch1* and *Gli1* was evaluated by qRT–PCR in six primary tumours obtained from *SmoM2* mice compared to wild-type mouse muscle, and up-regulation of *Ptch1* and *Gli1* in tumours supported activation of HH signalling consistent with activation of *SmoM2* (Figure 1E).

Histopathologically, *SmoM2* tumours exhibited a highly differentiated myogenic phenotype and lacked cellular atypia (Figure 2). They contained numerous 'myofibre-like', multinucleated, elongated cells as well as small round cells with uniform appearance, ovoid nuclei and evenly distributed chromatin. Tumour cells expressed myogenic markers, including the myogenic regulator factors myogenin and MyoD (normally expressed in activated satellite cells and proliferating myoblasts [12]), and exhibited uniformly high levels of the late myogenic differentiation markers desmin and actin (Figure 2). Ki67 indices were variable, including extremely low Ki67 indices in many tumours (19.1 ± 15.9%; range 3.4–41.8%). When we reviewed *SmoM2* tumour histology (n = 15 tumours) and myogenic marker staining (n = 8 tumours) in the context of human pathology conventions, *SmoM2* tumours consistently showed more prominent cytodifferentiation and less nuclear atypia than expected in embryonal rhabdomyosarcomas. It was also noted that *SmoM2* tumours bear close resemblance to human FRMs, rare benign tumours with muscle differentiation.

Human FRMs

Six FFPE FRMs were identified in the pathology archives at Boston Children's Hospital and the Brigham and Women's Hospital, Boston, MA (Figure 3; see also supplementary material, Table S1). All six patients were male, age at diagnosis was 0–108 months and four of six tumours were located at head/neck sites. Notably, two tumours arose in the postauricular area, which is a frequent site of origin of FRMs (Figure 3B). For FRM4, a previously described germline polymorphism at the *PTCH1* locus had been detected [Thr1195Ser, present in > 1% of the population, according to the Exome Variant Server, NHLBI Exome Sequencing Project (ESP), Seattle, WA, USA; accessed August 2012]. No information on germline mutational status was available for the other tumours. Clinical and outcome data were available for three of the six cases (FRM4-6, Figure 3B). These three patients had no family history of nevoid basal cell carcinoma syndrome (NBCCS), did not meet clinical criteria for NBCCS, had their tumours removed surgically, did not receive chemotherapy and/or radiation and were disease-free at 17 months–12 years after initial diagnosis. One patient (FRM4) had two local recurrences, both of which were resected (Figure 3B).

Mutational spectrum of human FRMs

We used hybrid-capture and targeted Illumina sequencing (OncoPanel v. 1) to investigate the molecular underpinnings of human FRMs, using DNA obtained from five FFPE tumour specimens (FRM2-6, Figure 3B). FRM1 yielded insufficient amounts of DNA and was discarded from the sequencing analysis. Normal corresponding tissue was available for tumours FRM5 (CONO5, muscle) and FRM6 (CONO6, lymph node). Three normal human muscle specimens obtained from donors without tumour history were also sequenced (NO1-3). We identified 10–17 SNVs in each of tumours FRM2–6 [non-synonymous, not present in normal muscle samples NO1-3, listed in the Exome Variant Server, NHLBI Exome Sequencing Project (ESP), Seattle, WA, USA, with a population frequency < 1%] (see supplementary material, Table S2). All 10–13 SNVs detected in tumours FRM5–6 were present in corresponding normal tissue (germline). All 15–17 SNVs detected in tumours FRM2–4 had indeterminate germline status. We also identified one to three insertions/deletions (indels; detected in > 25% of alleles) in tumours FRM2, FRM3, FRM4 (germline

status indeterminate) and FRM6 (germline status somatic) (see supplementary material, Table S3). In addition to SNVs and indels, there was clear indication of deletion of *PTCH1* and *FANCC*, which are co-located on chromosome 9, in samples FRM4 and FRM5 (Figure 4A, B, deleted regions marked by a red circle). For FRM5, the deleted region spanned Chr9, 95178901–98244322. Within this region, our targeted sequencing approach covered 1 exon of *CENPP*, all exons of *FANCC* and all exons of *PTCH1* except exon 3. All exons within this region were different from the genome mean by four or five standard deviations (SDs; in log2 space, except *PTCH1* exon 18). For FRM4, the deleted region spanned Chr9, 97873745–98248156. Within this region, OncoPanel v. 1 covered all exons of *FANCC* and *PTCH1*. All exons differed from the genome mean by six to eight SDs (in log2 space).

Several abnormalities were seen in more than one of the FRM specimens surveyed: First, indels in epithelial splicing regulatory protein 1 (*ESPR1*) were detected in three tumours, resulting in codon deletions in two tumours (FRM2, FRM4) and a frameshift mutation in one tumour (FRM3) (Table S3). Second, abnormalities in Fanconi anaemia complementation group C (*FANCC*) were present in three tumours, including two tumours with *FANCC* deletions (FRM4, FRM5) and one tumour with a *FANCC* SNV (FRM3) (Table S2, Figure 4). Third, missense mutations in the nuclear membrane protein spectrin repeat-containing nuclear envelope 1 (*SYNE1*) were detected in three tumours (FRM3, FRM5, FRM6) (Table S2). Finally, aberrations in HH pathway genes were found in three of five tumours, including two tumours with large deletions at the *PTCH1* locus (FRM4, FRM5) and one tumour with a *PTCH1* indel and a *SMO* SNV (FRM3) (Table 1, Figure 4; see also supplementary material, Tables S2, S3). The *SMO* mutation was previously found in 0.9% of the general population (according to the Exome Variant Server, NHLBI Exome Sequencing Project (ESP), Seattle, WA, USA). The *PTCH1* Indel caused a frameshift and thus represented a high-impact aberration. No *SUFU* or *HIP1* mutations were detected.

HH pathway gene aberrations in human FRMs

Our sequencing studies identified aberrations in *PTCH1* and *SMO* in three of five human FRMs sequenced (Table 1). FISH testing of *PTCH1* was performed on FFPE sections obtained from tumours FRM4–6 and normal tissue specimens (NO1-3), using a custom-made probe for *PTCH1* (labelled with spectrum orange) and a commercial probe for *CEP9* (labelled with spectrum green) (Figure 5). For tumour FRM3, there was no remaining tissue or DNA available to verify the abnormalities noted by OncoPanel v. 1 sequencing. The frequency of hybridization signal patterns in the *PTCH1* region was first analysed in the three normal tissue specimens (NO1-3). Heterozygous deletion patterns were observed in 11–37 of 100 cells, with a cut-off of 49 of 100 (determined as mean ± two SDs); homozygous deletion patterns (zero red and one green signal, or zero red and two green signals) were not observed in normal tissues. For all three tumours, heterozygous deletion patterns were within the range observed in normal tissues and did not exceed the cutoff. No homozygous deletion patterns were observed in tumour FRM6. However, homozygous deletion of *PTCH1* was noted in tumours FRM4 and FRM5 (homozygous deletion patterns in 73/100 and 76/100 cells, respectively) (Figure 5). This is consistent with the results of our sequencing studies, demonstrating deletions at the *PTCH1* locus in FRM4 and FRM5.

Discussion

This study was motivated by our observation that HH-driven myogenic tumours in mice with hyperactive HH signalling due to expression of an activated *SmoM2* allele resemble human FRMs. We evaluated the mutational spectrum of five human FRMs and noted functionally relevant aberrations in three of five human FRMs. Of note, Tostar *et al* previously reported a germline frameshift mutation and a somatic in-frame deletion at the

PTCH1 locus in a FRM diagnosed in a woman with NBCCS [13]. These findings suggest that activated HH signalling is a driving force behind the development of human FRMs.

Two of three FRMs with *PTCH1* aberrations carried mutations of indeterminate germline status (FRM3, FRM5). For FRM4, a germline *PTCH1* SNV had been detected. This SNV was previously linked to NBCCS [14], but subsequently found to be present in > 1% of the general population and reclassified as a non-pathogenic polymorphism. Patient FRM4 did not meet clinical criteria for NBCCS at the age of 10 years [15] but, interestingly, he experienced two local recurrences of his FRM. As multifocal rhabdomyomas were previously described in NBCCS [8], it is conceivable that the germline *PTCH1* variant in patient FRM4 contributed to the development of these tumours. We also note that our FISH studies demonstrated homozygous *PTCH1* loss in FRM4 and FRM5. This could be consistent with tumour development as a consequence of the combined effects of a somatic mutation in one allele and a germline lesion in the other.

We did not detect abnormalities in HH pathway genes in two of five tumours evaluated. It is possible that certain mutations in HH pathway genes were missed, due to the limited quality of the DNA obtained from > 10 year-old FFPE specimens or due to our sequencing approach (covering coding regions only). Alternatively, activated HH signalling may only contribute to a subset of human FRMs. For example, we also noted mutations in *ESPR1*, *FANCC* and SYNE1 in three FRMs each. *ESPR1* encodes a splicing factor that regulates the formation of epithelial cell-specific isoforms and has been linked to epithelial–mesenchymal transition [16]. *FANCC* encodes a DNA repair protein [17]. *SYNE1* encodes a nuclear membrane protein that has intracellular scaffold and linker functions [18]. Neither of these genes was previously linked to the biology of rhabdomyomas or rhabdomyosarcomas.

Multifocal muscle tumours in *SmoM2* mice do not metastasize to the lungs of tumour-bearing animals and have a highly differentiated myogenic phenotype. Similarly, low Ki67 indices and highly myogenic transcriptional profiles were previously observed in $Ptch^{+/-}$ mouse rhabdomyosarcomas [19]. We here note marked similarities in the histopathological presentation of *SmoM2* tumours and human FRM. Human FRMs are highly differentiated myogenic tumours that do not cause regional and/or systemic metastases. However, they can be difficult to distinguish from highly differentiated non-alveolar rhabdomyosarcoma [7]; Kodet *et al* previously remarked that it might be difficult to draw a sharp line between highly differentiated rhabdomyosarcomas and FRMs [9,11]. Interestingly, two of 15 tumours in a previously published case series of embryonal rhabdomyosarcomas with advanced differentiation resembled FRM; they consisted of almost entirely mature rhabdomyoblasts, interspersed with clusters of undifferentiated cells [20]. The question arises as to whether highly differentiated, rhabdomyoma-like non-alveolar rhabdomyosarcomas and human FRMs represent a biologically distinct category of myogenic tumours resulting from hyperactive HH signalling, or whether they are separate and distinct entities.

The presence of mutations in HH pathway genes in rhabdomyosarcoma tissue has been investigated previously. Somatic mutations in *PTCH1* were detected in seven non-alveolar rhabdomyosarcomas by FISH [13,21]. However, published studies aimed at determining the frequency of HH pathway gene mutations in rhabdomyosarcoma did not consider the degree of morphological differentiation within the spectrum of non-alveolar rhabdomyosarcoma and did not detect pathogenic mutations in *PTCH1*. It will be interesting to evaluate the presence of HH pathway gene mutations and expression patterns (including *PTCH1*) in highly differentiated, ‘rhabdomyoma-like’ rhabdomyosarcomas in order to directly address the question of whether highly differentiated RMS and FRM represent a biologically distinct

category and/or a spectrum of tumours with inactivating mutations in *PTCH1* (which could serve as a biomarker to facilitate diagnosis).

Supplementary Material

Refer to Web version on PubMed Central for supplementary material.

Acknowledgments

We thank C Namgyal, T Bowman and C Unitt in the DF/HCC research pathology core for help with DNA isolation and IHC; C Zhang and R Lee in the DF/HCC cytogenetics core for *PTCH1* FISH testing; R Ehrlich, M Ducar, A Sunkavalli and M Hanna in the DFCI Center for Cancer Genome Discovery (CCGD) for assistance with OncoPanel v. 1 sequencing; and D Tchessalova for animal colony maintenance/technical assistance. MuTect was made available through the generosity of Kristian Cibulskis and the Cancer Genome Analysis Program at the Broad Institute, Inc. This work was funded in part by the Harvard Stem Cell Institute, the National Institutes of Health (NIH; Grant Nos NIH DP2 OD004345 to AJW and NIH NS033642 to APM) and PALS Bermuda/St. Baldrick's and the Alex's Lemonade Stand Foundation (to SH). Content is solely the responsibility of the authors and does not necessarily represent the official views of the NIH or other funding agencies.

Abbreviations

ESP	Exome Sequencing Project
ESPR1	epithelial splicing regulatory protein 1 (human)
FANCC	Fanconi anaemia complementation group C (human)
FFPE	formalin-fixed, paraffin-embedded
FISH	fluorescence *in situ* hybridization
FRM	fetal rhabdomyoma
HH	Hedgehog
HIP1	Hedgehog interacting protein 1 (human)
Hip1	Hedgehog interacting protein 1 (mouse)
indel	insertion/deletion
NED	no evidence of disease
NBCCS	nevoid basal cell carcinoma syndrome
NHLBI	National Heart, Lung, and Blood Institute
PCR	polymerase chain reaction
Ptch1	Patched 1 (mouse)
PTCH1	PATCHED1 (human)
SMO	SMOOTHENED (human)
Smo	Smoothened (mouse)
SNV	single nucleotide variant
SUFU	suppressor of fused (human)
SYNE1	spectrin repeat containing, nuclear envelope 1 (human)

References

1. Ingham PW, McMahon AP. Hedgehog signaling in animal development: paradigms and principles. Genes Dev. 2001; 15:3059–3087. [PubMed: 11731473]
2. Chari NS, McDonnell TJ. The sonic hedgehog signaling network in development and neoplasia. Adv Anat Pathol. 2007; 14:344–352. [PubMed: 17717435]
3. Corcoran RB, Scott MP. A mouse model for medulloblastoma and basal cell nevus syndrome. J Neurooncol. 2001; 53:307–318. [PubMed: 11718263]
4. Mao J, Ligon KL, Rakhlin EY, et al. A novel somatic mouse model to survey tumorigenic potential applied to the Hedgehog pathway. Cancer Res. 2006; 66:10171–10178. [PubMed: 17047082]
5. Hahn H, Wojnowski L, Zimmer AM, et al. Rhabdomyosarcomas and radiation hypersensitivity in a mouse model of Gorlin syndrome. Nat Med. 1998; 4:619–622. [PubMed: 9585239]
6. Gerber AN, Wilson CW, Li YJ, et al. The hedgehog regulated oncogenes Gli1 and Gli2 block myoblast differentiation by inhibiting MyoD-mediated transcriptional activation. Oncogene. 2007; 26:1122–1136. [PubMed: 16964293]
7. Kapadia SB, Meis JM, Frisman DM, et al. Fetal rhabdomyoma of the head and neck: a clinicopathologic and immunophenotypic study of 24 cases. Hum Pathol. 1993; 24:754–765. [PubMed: 8319954]
8. Klijanienko J, Caillaud JM, Micheau C, et al. Basal-cell nevomatosis associated with multifocal fetal rhabdomyoma. A case. Presse Med. 1988; 17:2247–2250. [PubMed: 2974590]
9. Kodet R, Fajstavr J, Kabelka Z, et al. Is fetal cellular rhabdomyoma an entity or a differentiated rhabdomyosarcoma? A study of patients with rhabdomyoma of the tongue and sarcoma of the tongue enrolled in the intergroup rhabdomyosarcoma studies I, II, and III. Cancer. 1991; 67:2907–2913. [PubMed: 2025857]
10. Dahl I, Angervall L, Save-Soderbergh J. Foetal rhabdomyoma. Case report of a patient with two tumours. Acta Pathol Microbiol Scand A. 1976; 84:107–112. [PubMed: 1251730]
11. Jacques SM, Lawrence WD, Malviya VK. Uterine mixed embryonal rhabdomyosarcoma and fetal rhabdomyoma. Gynecol Oncol. 1993; 48:272–276. [PubMed: 8428702]
12. Rudnicki MA, Le Grand F, McKinnell I, et al. The molecular regulation of muscle stem cell function. Cold Spring Harb Symp Quant Biol. 2008; 73:323–331. [PubMed: 19329572]
13. Tostar U, Malm CJ, Meis-Kindblom JM, et al. Deregulation of the hedgehog signalling pathway: a possible role for the *PTCH* and *SUFU* genes in human rhabdomyoma and rhabdomyosarcoma development. J Pathol. 2006; 208:17–25. [PubMed: 16294371]
14. Boutet N, Bignon YJ, Drouin-Garraud V, et al. Spectrum of *PTCH1* mutations in French patients with Gorlin syndrome. J Invest Dermatol. 2003; 121:478–481. [PubMed: 12925203]
15. Lo Muzio L. Nevoid basal cell carcinoma syndrome (Gorlin syndrome). Orphanet J Rare Dis. 2008; 3:32. [PubMed: 19032739]
16. Reinke LM, Xu Y, Cheng C. Snail represses the splicing regulator epithelial splicing regulatory protein 1 to promote epithelial–mesenchymal transition. J Biol Chem. 2012; 287:36435–36442. [PubMed: 22961986]
17. Yuan F, Song L, Qian L, et al. Assembling an orchestra: Fanconi anemia pathway of DNA repair. Front Biosci. 2010; 15:1131–1149.
18. Rajgor D, Mellad JA, Autore F, et al. Multiple novel nesprin-1 and nesprin-2 variants act as versatile tissue-specific intracellular scaffolds. PLoS One. 2012; 7:e40098. [PubMed: 22768332]
19. Kappler R, Bauer R, Calzada-Wack J, et al. Profiling the molecular difference between Patched- and p53-dependent rhabdomyosarcoma. Oncogene. 2004; 23:8785–8795. [PubMed: 15480423]
20. Kodet R, Newton WA Jr, Hamoudi AB, et al. Orbital rhabdomyosarcomas and related tumors in childhood: relationship of morphology to prognosis—an Intergroup Rhabdomyosarcoma study. Med Pediatr Oncol. 1997; 29:51–60. [PubMed: 9142207]
21. Bridge JA, Liu J, Weibolt V, et al. Novel genomic imbalances in embryonal rhabdomyosarcoma revealed by comparative genomic hybridization and fluorescence *in situ* hybridization: an intergroup rhabdomyosarcoma study. Genes Chromosomes Cancer. 2000; 27:337–344. [PubMed: 10719362]

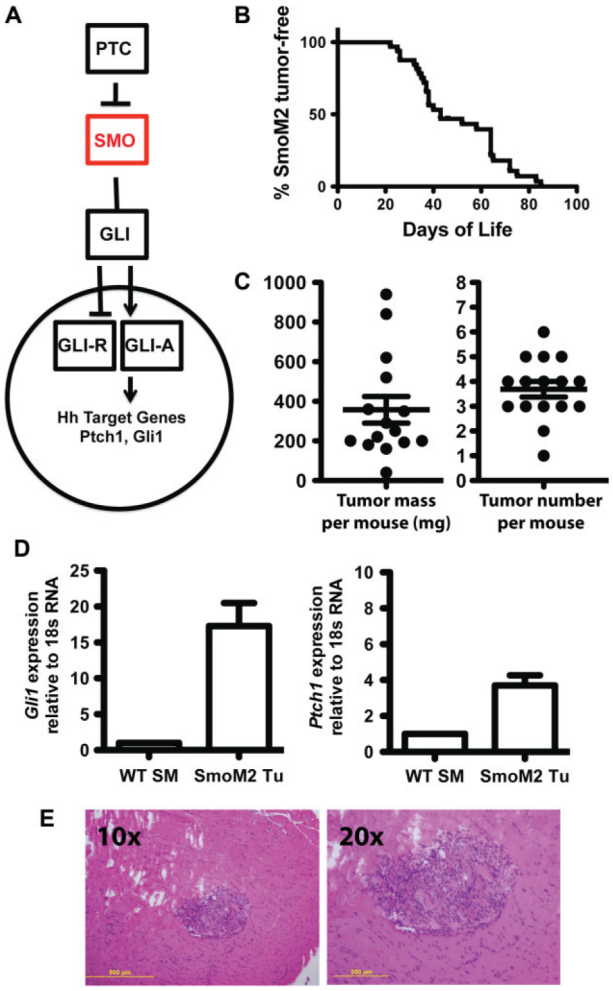

Figure 1.

SmoM2 myogenic tumours in *R26-SmoM2;CAGGS-CreER* mice. (A) Constitutive activation of HH pathway signalling; Gli-R, Gli repressor; Gli-A, Gli-activating complex. (B) *R26-SmoM2;CAGGS-CreER* mice develop myogenic tumours with high penetrance within the first 3 months of life. (C) SmoM2 myogenic tumours are multifocal and reach a total tumour mass of 358 ± 67 mg/mouse. (D) Increased expression of HH target genes *Ptch1* and *Gli1* in SmoM2 tumours compared to wild-type (WT) mouse muscle (SM) reflects activated HH signalling in SmoM2 myogenic tumours (mean ± SD of six SmoM2 tumours and three muscle specimens). (E) Random muscle sections obtained from *R26-SmoM2;CAGGS-CreER* mice contain small tumour foci. Images were taken at ×10 and ×20 magnification.

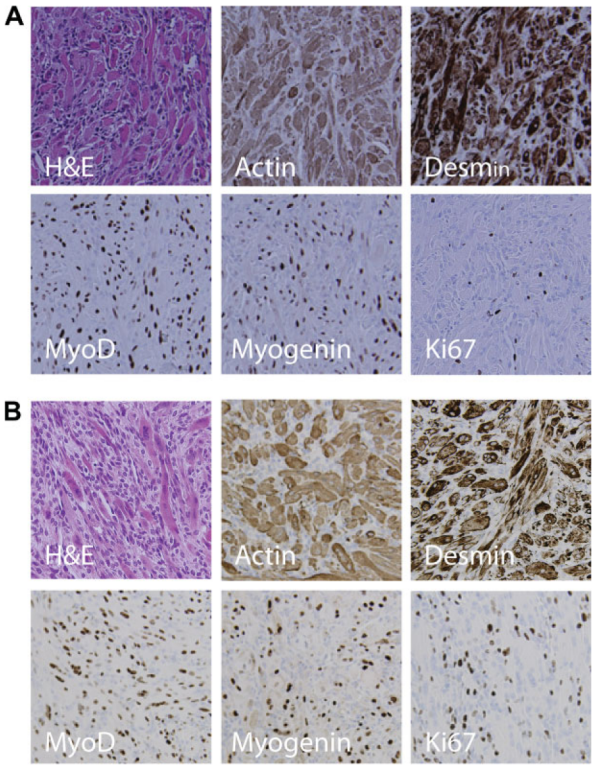

Figure 2.
Morphological and immunohistochemical (IHC) evaluation of SmoM2 tumours: H&E and IHC staining against Actin, Desmin, MyoD, Myogenin and Ki67. Representative images are shown for tumours originating in 56 day-old (A) and 27 day-old (B) *R26-SmoM2;CAGGS-CreER* mice; images were taken at ×20 magnification.

A

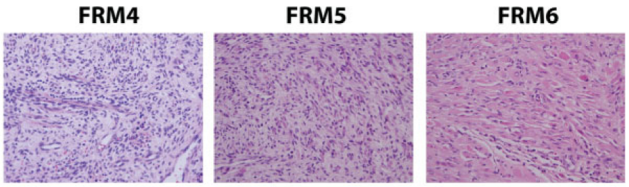

B

Tumour ID	Gender	Age at diagnosis (months)	Tumour location	Outcome
FRM1	Male	96	chest wall	unknown
FRM2	Male	4	tongue	unknown
FRM3	Male	108	chest wall	unknown
FRM4	Male	0	left postauricular	2 recurrences, NED 12 years post diagnosis
FRM5	Male	0	left postauricular	0 recurrences, NED 17 months post diagnosis
FRM6	Male	14	infratemporal fossa	0 recurrences, NED 10 years post diagnosis

Figure 3.

Human fetal rhabdomyomas (FRMs). Six human FRM specimens were identified. (A) Representative images of H&E-stained sections of tumours FRM4, FRM5 and FRM6 are shown; images were taken at ×40 magnification. (B) All patients were male; age at diagnosis was 0–108 months, and four of six tumours were located in the head/neck region. Clinical and outcome data were available for three of six cases (FRM4–6). These three patients did not meet clinical criteria for NBCCS and were tumour-free 17 months–12 years post-diagnosis. No evidence of disease, NRD.

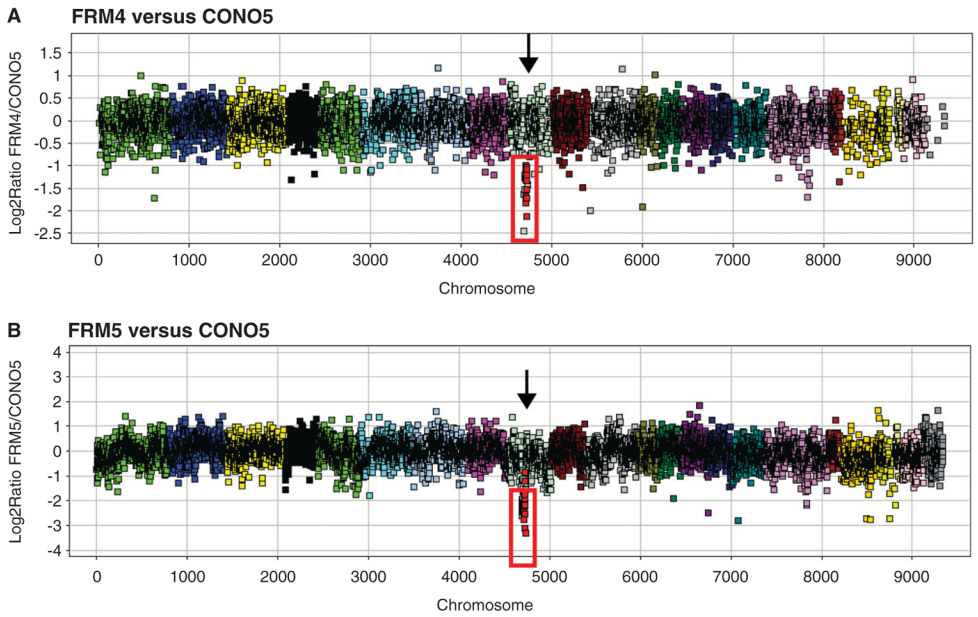

Figure 4.

PTCH1 copy number variations in human fetal rhabdomyomas (FRMs). Ratio of sequence coverage (log2 scale) of tumours FRM4 (A) and FRM5 (B) against CONO5, showing a deletion of *FANCC* and *PTCH1* on chromosome 9 (marked by the red circle). For FRM5, the deleted region spanned Chr9, 95178901–98244322. Within this region, OncoPanel v. 1 covered one exon of *CENPP*, all exons of *FANCC* and all exons of *PTCH1* except exon 3. All the exons except *PTCH1* exon 18 were four to five SDs different from the genome mean (in log2 space). For FRM4, the deleted region spanned Chr9, 97873745–98248156. Within this region, OncoPanel v. 1 covered all exons of *FANCC* and *PTCH1*. All the exons were six to eight SDs different from the genome mean (in log2 space).

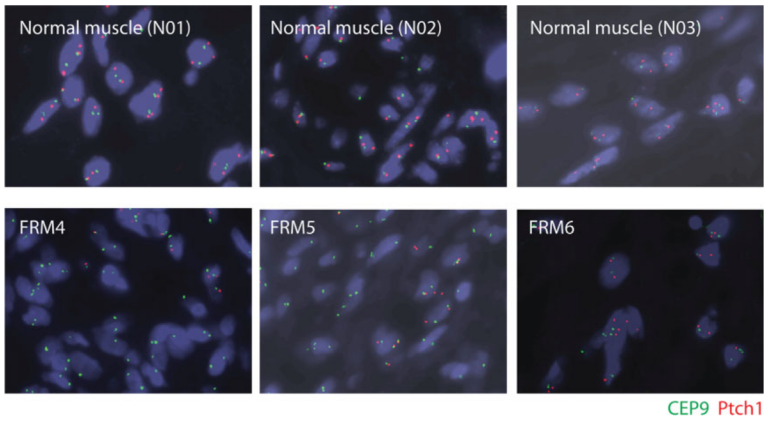

Figure 5.

PTCH1 deletion in human fetal rhabdomyomas (FRM). Fluorescence *in situ* hybridization testing of *PTCH1* revealed homozygous deletion of *PTCH1* in tumours FRM4 (lower left panel) and FRM5 (lower middle panel), consistent with large deletions at the *PTCH1* locus noted by sequencing. *PTCH1* expression in tumour FRM6 (lower right panel) was normal, without evidence of homozygous deletion patterns. Heterozygous deletion patterns in tumours FRM4–6 were within the range observed in normal muscle specimens (upper panels).

Table 1

Aberrations in Hedgehog pathway genes in fetal rhabdomyomas

	PTCH1	*SMO*	*SUFU*	*HIP1*
FRM2	–	–	–	g.75172270G > A (p.P930P)
FRM3	**g.98,220,305 GC > G**	g.128845511G > A (p.V270I)	–	–
FRM4	**Homozygous deletion***	–	–	–
FRM5	**Homozygous deletion***	–	–	–
FRM6	_*	–	–	–

Functionally relevant aberrations are marked in bold. *PTCH1* indel 98,220,305 GC > G represents a frameshift mutation. *SMO* p.V270I is present in > 1% of the population. *HIP1* p.P930P was predicted to be silent.

* Presence or lack of deletion was confirmed by FISH (Figure 5).